Accepted Manuscript

Selective hydroxylation of 1,8- and 1,4-cineole using bacterial P450 variants

Joel H.Z. Lee, Siew Hoon Wong, Jeanette E. Stok, Sarah A. Bagster, James Beckett, Jack K. Clegg, Aidan Brock, James J. De Voss, Stephen G. Bell

PII: S0003-9861(18)30673-8

DOI: https://doi.org/10.1016/j.abb.2018.12.025

Reference: YABBI 7900

To appear in: *Archives of Biochemistry and Biophysics*

Received Date: 29 August 2018

Revised Date: 24 October 2018

Accepted Date: 21 December 2018

Please cite this article as: J.H.Z. Lee, S.H. Wong, J.E. Stok, S.A. Bagster, J. Beckett, J.K. Clegg, A. Brock, J.J. De Voss, S.G. Bell, Selective hydroxylation of 1,8- and 1,4-cineole using bacterial P450 variants, *Archives of Biochemistry and Biophysics* (2019), doi: https://doi.org/10.1016/j.abb.2018.12.025.

Selective hydroxylation of 1,8- and 1,4-cineole using bacterial P450 variants

Joel H. Z. Lee[a], Siew Hoon Wong[b], Jeanette E. Stok[b], Sarah A. Bagster[a], James Beckett[b], Jack K. Clegg[b], Aidan Brock[b], James J. De Voss[b] and Stephen G. Bell[a]

[a] *Department of Chemistry, School of Physical Sciences, University of Adelaide, Adelaide, SA 5005, Australia*

[b] *Department of Chemistry, School of Chemistry and Molecular Biosciences, University of Queensland, St. Lucia, Brisbane QLD 4072, Australia*

Dr Stephen G. Bell

E-mail: stephen.bell@adelaide.edu.au

Prof. James J. De Voss

E-mail: j.devoss@uq.edu.au

Abstract

This study has evaluated the use of the P450 metalloenzymes CYP176A1, CYP101A1 and CYP102A1, together with engineered protein variants of CYP101A1 and CYP102A1, to alter the regioselectivity of 1,8- and 1,4-cineole hydroxylation. CYP176A1 was less selective for 1,4-cineole oxidation when compared to its preferred substrate, 1,8-cineole. The CYP102A1 variants significantly improved the activity over the WT enzyme for oxidation of 1,4- and 1,8-cineole. The CYP102A1 R47L/Y51F/A74G/F87V/L188Q mutant generated predominantly (1*S*)-6α-hydroxy-1,8-cineole (78% e.e.) from 1,8-cineole. Oxidation of 1,4-cineole by the CYP102A1 R47L/Y51F/F87A/I401P variant generated the 3α product in >90% yield. WT CYP101A1 formed a mixture metabolites with 1,8-cineole and very little product was generated with 1,4-cineole. In contrast the F87W/Y96F/L244A/V247L and F87W/Y96F/L244A variants of CYP101A1 favoured formation of 5α-hydroxy-1,8-cineole (>88%, 1*S* 86% e.e.) while the F87V/Y96F/L244A variant generated (1*S*)-6α-hydroxy-1,8-cineole in excess (90% regioselective, >99% e.e.). The CYP101A1 F87W/Y96F/L244A/V247L and F87W/Y96F/L244A mutants improved the oxidation of 1,4-cineole generating an excess of the 3α metabolite (1*S* >99% e.e. with the latter). The CYP101A1 F87L/Y96F variant also improved the oxidation of this substrate but shifted the site of oxidation to the isopropyl group, (8-hydroxy-1,4-cineole). When this 8-hydroxy metabolite was generated in significant quantities desaturation of C8-C9 to the corresponding alkene was also detected.

Graphical Abstract

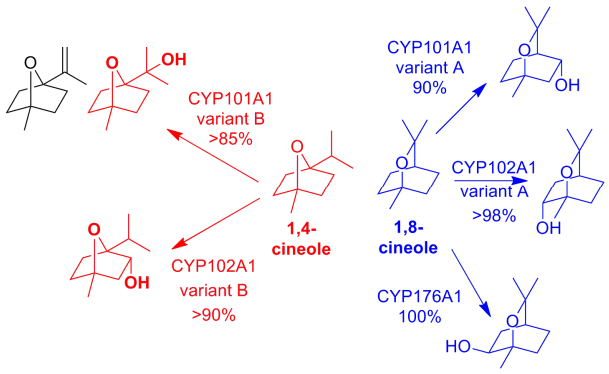

Highlights

CYP176A1 was less selective for 1,4-cineole oxidation compared to 1,8-cineole.

CYP102A1 and CYP101A1 variants were used to generate (1*S*)-6α-hydroxy-1,8-cineole in excess (>90%).

Other mutant forms of CYP101A1 were selective for 5α-hydroxy-1,8-cineole (>88%, 86% e.e.).

Oxidation of 1,4-cineole by CYP102A1 and CYP101A1 mutants generated the 3α product in >90% yield.

The CYP101A1 F87L/Y96F variant favoured 8-hydroxy-1,4-cineole formation.

The formation of 8-hydroxy-1,4cineole was accompanied by desaturation to a C8-C9 alkene.

Keywords: enzyme catalysis; cytochrome P450; cineole; hydroxylation, C-H bond oxidation

1. Introduction

The monoterpenoid group of natural products are widespread, abundant and structurally diverse, and these attributes correlate with a wide range of biological functions [1, 2]. They make up the major proportion of many essential oils and have uses as flavours, fragrances and pheromones [1, 3, 4]. They also show antimicrobial and medicinal properties and have uses as pesticides, herbicides and components of pharmaceuticals [5, 6]. The parent monoterpenes are often easily accessible from natural oils but the hydroxylated or oxyfunctionalised forms usually occur in lower amounts [3, 7].

The monoterpene 1,8-cineole **1** (1,3,3-trimethyl-2-oxabicyclo[2,2,2]octane) is the major component of eucalyptus oil, while 1,4-cineole **2** (4-methyl-1-propan-2-yl-7-oxabicyclo[2.2.1]heptane) is found in some plant oils and is also present in lime juice (Fig. 1) [8-10]. Both cineoles are achiral but a single hydroxylation usually leads to the generation of at least two stereogenic centres. The oxygenated derivatives of both are important chiral synthons, intermediates in the synthesis of herbicides (e.g. cinmethylin), antimicrobials and fragrances [7, 9, 11-20]. The chemical synthesis of hydroxylated cineole analogues is difficult and requires the use of highly reactive, non-environmentally friendly reagents that usually generate a mixture of racemic products. The use of metalloenzyme biocatalysts to selectively introduce oxygen into selected C-H bonds of the parent cineoles is very attractive as it would allow these reactions to be performed in a single step under ambient conditions [21-23].

There has been increasing attention to the use of metalloenzymes as biocatalysts for the discovery of new routes for the synthesis of hydroxylated terpene analogues for the production of antimicrobial and bactericidal agents or for the fragrance industry [5, 6, 24]. Of particular interest is the ability of such enzymes, especially the cytochromes P450

(P450s), to synthesise specific oxygenated molecules in a highly regio- and enantioselective fashion.

The P450s are a superfamily of hemoprotein monooxygenases that are involved in hydroxylation, epoxidation, heteroatom dealkylations and other, more complex reactions [25-27]. The majority of P450 enzymes utilise a reactive high-valent iron-oxo radical cation intermediate, compound I (Cpd I), to insert one oxygen atom from dioxygen into unactivated carbon-hydrogen bonds. The catalytic cycle of the enzyme involves multiple steps. After initial substrate binding, the first electron transfer step reduces the ferric iron to the ferrous form. The electrons required for this and a subsequent reduction step are usually sourced from a nicotinamide cofactor (NADH or NADPH) and delivered via electron transfer proteins [28-30]. Oxygen rapidly binds to the ferrous form and is then activated by a second electron. Protein controlled delivery of protons facilitates dioxygen bond cleavage with generation of the reactive intermediate, Cpd I [31]. The pathway of the oxygen insertion reaction by Cpd I is accounted for by the radical rebound mechanism [32, 33]. In general, bacterial P450 enzymes tend to have an active site architecture that holds the physiological substrate in such a way that carbon-hydrogen bond hydroxylation occurs with high regio-, stereo-, and enantioselectivity. The ability of these enzymes to catalyse this reaction under ambient conditions offers advantages over traditional multistep or unselective organic synthesis routes [34-36]. Hence, the bacterial P450 enzymes, which are often soluble, highly active and selective, are well suited for biocatalytic applications [34-36]. P450s such as CYP101A1 ($P450_{cam}$), CYP102A1 ($P450_{BM3}$) and CYP176A1 ($P450_{cin}$) have previously demonstrated their utility in catalysing the oxidation of a number of terpenes and are therefore, ideal candidates for exploring the oxidation products that could be generated from 1,8- and 1,4-cineole [24, 37-41].

CYP176A ($P450_{cin}$) is an example of a bacterial P450 that has been shown to catalyse the enantiospecific hydroxylation of 1,8-cineole **1** to produce (1*R*)-6β-hydroxycineole **3a** (Scheme 1, Fig. 2). This P450 was initially identified in a bacterium thought to be *Citrobacter braakii* along with its redox partners, which included the FMN containing flavodoxin, cindoxin (Cdx) [42, 43]. When reconstituted with *Escherichia coli* flavodoxin reductase it is an NADPH dependent P450 system that efficiently catalyses the enantiospecific hydroxylation of 1,8-cineole [42, 44]. This is the first step in the biodegradation of cineole by the bacterium which can use this monoterpene as it sole source of carbon and energy [15]. Mutagenesis studies have demonstrated that a range of hydroxycineole isomers can be obtained from a number of single amino acid mutations of CYP176A1 around the heme containing active site (Fig. 2) [45-47]. In addition, CYP176A1 is able to catalyse the less selective oxidation of other monoterpenes, such as both enantiomers of camphor [24, 43]. An *in vivo* system, comprising of $P450_{cin}$ and Cdx and the endogenous *E. coli* flavodoxin was constructed to enable larger scale metabolite generation using intact cells [24].

The bacterial monooxygenase CYP101A1 ($P450_{cam}$), from *Pseudomonas putida*, catalyses the stereospecific hydroxylation of (1*R*)-camphor to 5-*exo*-hydroxycamphor (Fig. 2) [34, 48]. This oxidation, like that of 1,8-cineole by CYP176A1, is the first step in the utilisation of the substrate as an energy source by the bacterium. It obtains its electrons from NADH via a class I electron transfer system, comprising an FAD containing flavoprotein, putidaredoxin reductase, and a [2Fe-2S] ferredoxin, putidaredoxin [49, 50]. The WT enzyme has a limited substrate range outside of camphor but can oxidise other monoterpenes including 1,8-cineole, which is hydroxylated less selectively to (1*S*)-6α-hydroxycineole **3b** and both enantiomers of 5α- and 5β-hydroxycineole **3c-d** (Scheme 1) [40]. Mutations at residues in the active-site of CYP101A1 have been found to improve its affinity, activity and

selectivity toward other substrates, e.g. the monoterpenes (*S*)-limonene and (+)-α-pinene (Fig. 2) [34, 37, 39, 51-56]. The enzyme has also been altered to oxidise substrates as varied as small chain alkanes (<C5) and polycyclic aromatic hydrocarbons as large as pyrene [37, 39, 52, 55, 57-61].

The P450 CYP102A1 ($P450_{BM3}$), which was found in *Bacillus megaterium*, is a fatty acid hydroxylase that oxidises fatty acid substrates close to the omega terminus (Fig. 2) [62-64]. This enzyme was the first example of a P450 in which the electron transfer partner domains are fused to the heme domain. Other members of the CYP102A subfamily have been found to have the same secondary structure properties [65-70] CYP102A1 has a high specificity for NADPH as the electron source,[71] and the enzyme has been shown to work as a dimer with very high monooxygenase activity [65-68, 72, 73]. It is soluble, easy to produce and the self-sufficient nature and high activity often make it the P450 of choice for biocatalytic applications. As such it has been used as a template for protein engineering and evolution studies to design efficient and selective oxidation biocatalysts [34, 39, 74-82]. CYP102A1 variants, which enhance the oxidation activity for unnatural substrates but do not alter the product regioselectivity have been identified [83-86]. Variants in which phenylalanine 87 and other residues in the enzyme active site have been modified, alter the substrate binding profile and product selectivity [76, 87-90]. For example, the GVQ variant (A74G/F87V/L188Q) of CYP102A1 has been reported to be a biocatalyst for the oxidation of hydrophobic organic molecules including alkyl napthalenes [83, 91]

The selective metalloprotein-catalyzed oxidation of cineoles to specific hydroxycineoles could generate new green chemistry routes to important molecules. Recently WT CYP101B1 from *Novosphingobium aromativicorans* was shown to generate predominantly (1*S*)-5α-hydroxy-1,8-cineole **3c** with high activity [40]. Others have reported new bacterial enzymes of the CYP101J subfamily from *Sphingobium yanoikuyae* B2, which

can oxidise 1,8-cineole to form (1*R*)-6α-hydroxy-1,8-cineole **3b** [92, 93]. Whole-cell microbial oxidation of 1,4-cineole **2** by *Streptomyces griseus* and other bacteria yielded mixtures of the 8- and 9-hydroxy-1,4-cineoles (**5a** and **5d**) and isomers from hydroxylation at the 2-position [12, 17, 18]. Here we report results of oxidation of 1,8- and 1,4-cineole using mutant forms of CYP102A1 and CYP101A1 in order to investigate the potential use of these metalloenzymes as selective biocatalysts in the generation of specific hydroxycineoles. Metabolites from the oxidation of 1,4-cineole by CYP176A1 are also identified. In addition, whole-cell oxidation of both cineoles was used to compare the activity and selectivity of the different P450 enzymes.

2. Experimental Section

2.1 General

General reagents, 1,8-cineole **1** and 1,4-cineole **2** were from Sigma-Aldrich. Buffer components, NADPH, and isopropyl-β-D-thiogalactopyranoside (IPTG) were from Astral Scientific (Australia) or VWR. Production and purification of full-length CYP102A1 variants for *in vitro* use were carried out as described previously [83, 94]. UV/Vis spectroscopy was performed on an Agilent Cary 60 spectrophotometer with temperature control at 30 °C. Gas chromatography mass spectrometry (GC-MS) analyses were carried out on a Shimadzu GC-2010 coupled to a GC-MS-QP2010S detector or a GC-17A coupled to a QP5050A MS detector. Both systems used a DB-5 MS fused silica column (30 m x 0.25 mm, 0.25 µm) and helium as the carrier gas. The GC retention times are given in the figure legends and the methods in the supplementary material. Additional GC analysis and enantioselective chromatography were performed on a Shimadzu Tracera GC coupled to Barrier discharge Ionization Detector (BID) detector using a Supelcowax column (30 m x 0.32 mm x 0.25 um) and a RT®-BDEXse chiral silica column (Restek; 30 m x 0.32 mm x 0.25 um), respectively. Enantioselective GC analysis of the cineole metabolites was performed on Cyclodextrin-B column (25 m × 0.25 mm) on a Shimadzu GC-17A equipped with an FID.

2.2 Activity assays

CYP102A1 *in vitro* NADPH turnovers were run at 30 °C in 1200 µL of 50 mM Tris, pH 7.4 at 30 °C, containing 0.2 µM enzyme and 120 µg bovine liver catalase. The buffer was saturated with oxygen gas just before use and the assays were allowed to equilibrate for 1 min prior to the addition of the appropriate cineole substrate (1 mM substrate from a 100 mM stock in DMSO). To initiate the reaction NADPH was added, from a 20 mg mL^{-1} stock, to a final concentration of ~320 µM (equivalent to 2 AU). A period of 10 seconds was

allowed to elapse after NADPH addition, to enable the rate of consumption to become linear, before the absorbance at 340 nm was monitored. The reactions were allowed to run until all the NADPH was consumed. The NADPH turnover rate was derived using ε_{340} = 6.22 mM^{-1} cm^{-1}.

2.3 *In vivo* metabolite generation and product identification

The CYP101A1 variants were screened using a plasmid system pCWSGB++ (pCWori+ based) which contained the genes for PdR, Pdx and the relevant mutant as described previously (Table S1) [37, 39, 51, 55, 57, 58]. CYP176A1 was screened using the biscistronic system (also in pCWori+) containing P450 enzyme and Cdx which is supported by the endogenous flavoprotein reductase of the *E. coli* [24, 95]. The plasmids transformed in *E. coli* (DH5α) cells and a single colony was grown in 2 x YT medium containing ampicillin (100 μg mL^{-1}) and the protein was produced by induction with IPTG [53]. After induction the cell pellet was harvested by centrifugation and resuspended in *E. coli* minimal medium (EMM; K_2HPO_4, 7 g, KH_2PO_4, 3 g, Na_3citrate, 0.5 g, $(NH_4)_2SO_4$, 1 g, $MgSO_4$, 0.1 g, 20% glucose, 20 mL and glycerol, 1% v/v per litre).

To isolate and identify the cineole products, and to compare the CYP102A1 turnovers a whole-cell oxidation system utilising the pET28 plasmid containing the CYP102A1 gene of interest was used. The plasmids were transformed into competent BL21(DE3) cells, grown in 2 x YT broth containing kanamycin (30 μg mL^{-1}). Protein generation was induced by addition of IPTG and the cultures were allowed to continue for 16 h before the cells were harvested by centrifugation. The cell pellet was washed and resuspended in EMM. The cineoles (2 mM from a 100 mM stock in ethanol) were added to the cells (50 ml in a 250 mL flask) the reactions were shaken at 150 rpm and 30 °C. A second aliquot of substrate was added after 6 hours and the reactions were allowed to

proceed for 16 hours. Aliquots of the turnover (1 mL) were taken and extracted with ethyl acetate for analysis by GC-MS.

The CYP101A1 and CYP102A1 variants were transformed into the *E. coli* strain BL21(DE3) and grown in LB with the relevant antibiotics (see above). The cells were harvested, the biomass yield was recorded as the cell wet weight, before they were resuspended in EMM (50 mL in 250 mL flask). The reactions were performed in duplicate and analysed as described below. The concentration of P450 was determined by lysing the cells (via sonication) and recording the CO difference spectrum of the supernatant [96].

2.4 Product analysis

After the NADPH consumption assays were completed with CYP102A1 variants or when analysing the whole-cell oxidation systems, 990 μL of the reaction mixture (including the cells in the case of whole-cell turnovers) was mixed with 10 μL of an internal standard solution (*p*-cresol, 20 mM stock solution in DMSO). The mixture was extracted with 400 μL of ethyl acetate and the organic extracts were used directly for GC-MS or GC analysis. Products were initially identified by matching the GC-MS mass spectra to those expected for the products (see supplementary material). To obtain the coupling efficiency products were calibrated against 1,8-cineole and 1.4-cineole using the assumption that isomeric products would give comparable responses.

The supernatant (50 mL) from an *in vivo* turnover of the cineoles was extracted with ethyl acetate (3 x 50 mL), washed with brine (50 mL). The organic extracts were pooled, dried with magnesium sulphate, filtered and the solvent was removed by vacuum distillation and then under a stream of nitrogen. The products were purified by silica gel chromatography using a hexane/ethyl acetate stepwise gradient. The composition of the fractions was assessed by TLC and GC-MS and those containing a single major product were combined for characterisation. The purified product was dissolved in $CDCl_3$ and the

organics characterised by NMR spectroscopy and GC-MS. When separation was not possible fractions were analysed by NMR and distinctive signals were matched to those of the metabolites reported in the literature. These NMR spectra were acquired on a Bruker AV at 500 MHz.

2.5 NMR and MS data for 1,4-cineole products

The distinctive NMR signals and MS fragmentation patterns used to characterise the 1,4-cineole derivatives are shown below. These were purified from *in vivo* turnovers with enzymes discussed in this work or synthesised from such compounds as described. The oxidised 1,8-cineole derivatives have been identified previously and were characterised by comparison to previous literature or authentic standards using methods which have been previously described [24, 40, 42, 46, 95].

8-hydroxy-1,4-cineole 5a [12, 97] (oil) lit [98].

^{1}H NMR ($CDCl_3$, 400 MHz): δ 1.25 (s, 6H, 9-CH_3 & 10-CH_3), 1.43 (s, 3H, 7-CH_3).

^{13}C NMR ($CDCl_3$, 100 MHz): δ 21.1, 25.3 (2 × CH_3), 31.9 (2 × CH_2), 37.5 (2 × CH_2), 71.6, 83.9, 91.7.

GC-MS (*m/z*): 170 (M^+, 7), 155 (4), 137 (7), 112 (13), 111 (39), 110 (18), 109 (12), 97 (10), 95 (9), 93 (15), 85 (13), 83 (8), 79 (9), 69 (17), 67 (12), 59 (100), 55 (19), 43 (96).

3β-hydroxy-1,4-cineole 5b [12] (oil, major component in a mixture).

^{1}H NMR ($CDCl_3$, 400 MHz): δ 0.91 & 1.00 (2 × dd, *J* = 6.9 & 0.7 Hz, 2 × 3H, 9-CH_3 & 10-CH_3), 1.45 (s, 3H, 7-CH_3), 1.70 (td, *J* = 12.2 & 3.4 Hz, 1H), 2.18 (dd, *J* = 13.3 & 6.9 Hz, 1H), 2.36 (septet, *J* = 6.9 Hz, 1H), 3.89 (ddd, *J* = 9.3, 6.8 & 2.0 Hz, 1H).

GC-MS (*m/z*): 170 (M^+, 7), 155 (1), 139 (1), 137 (3), 127 (8), 125 (6), 111 (8), 109 (8), 86 (54), 84 (43), 71 (58), 43 (100).

2β-hydroxy-1,4-cineole 5c [12] [13] (solid, major component in a mixture).

^{1}H NMR ($CDCl_3$, 400 MHz): δ 0.94 & 0.95 (2 × d, *J* = 6.9 Hz, 2 × 3H, 9-CH_3 & 10-CH_3), 1.40 (s, 3H, 7-CH_3), 2.04 (m, 2H), 3.73 (t, *J* = 7.5 Hz, 1H).

^{13}C NMR ($CDCl_3$, 100 MHz): δ 16.4, 18.18, 18.21, 32.60, 32.63, 32.9, 45.2, 76.9, 85.6, 88.8

GC-MS (*m/z*): 170 (M^+, 4), 153 (4), 137 (2), 127 (6), 125 (9), 112 (17), 109 (10), 97 (13), 95 (10), 86 (10), 83 (19), 71 (23), 43 (100).

9-hydroxy-1,4-cineole 5d [12, 97] (oil, mixture) [97].

^{1}H NMR ($CDCl_3$, 400 MHz): δ 0.83 (d, *J* = 7.0 Hz, 10-CH_3), 1.43 (s, 3H, 7-CH_3), 3.48 (dd, *J* = 11.2 & 4.2 Hz, 1H), 3.70 (dd, *J* = 11.1 & 9.6 Hz, 1H).

GC-MS (*m/z*): 170 (M^+, 14), 155 (1), 141 (11), 139 (12), 137 (3), 123 (13), 111 (38), 97 (10), 95 (18), 93 (17), 91 (7), 87 (35), 83 (15), 81 (13), 79 (19), 69 (29), 67 (28), 55 (52), 43 (100).

2α-hydroxy-1,4-cineole 5e [99] (oil, major component in a mixture from whole-cell oxidation system)

^{1}H NMR ($CDCl_3$, 400 MHz): δ 0.901 & 0.905 (2 × d, *J* = 6.9 Hz, 2 × 3H, 9-CH_3 & 10-CH_3), 1.37 (s, 3H, 7-CH_3), 1.93 (sept, *J* = 6.8 Hz, 1H), 2.05 (m, 1H), 2.28 (ddd, *J* = 12.3, 8.6, & 5.7 Hz, 1H), 3.90 (m, 1H)

GC-MS (*m/z*): 170 (M^+, 4), 153 (3), 140 (1), 137 (2), 127 (5), 125 (10), 112 (18), 111 (7), 97 (12), 95 (9), 83 (18), 81 (14), 71 (23), 58 (27), 43 (100)

3α-hydroxy-1,4-cineole 5f mp. 81 – 82 °C (lit. [100] mp. 56 °C); $[\alpha]_D^{23}$ 17° (*c* 0.14, $CHCl_3$), lit. [100] $[\alpha]_D$ 2.5° (*c* 0.5, $CHCl_3$).

^{1}H NMR ($CDCl_3$, 500 MHz): δ 0.98 & 0.99 (2 × d, *J* = 6.9 Hz, 2 × 3H, 9-CH_3 & 10-CH_3), 1.34 (s, 3H, 7-CH_3), 1.38 (dd, *J* = 12.5 & 3.1 Hz, 1H, 2-CH), 1.46 – 1.59 (m, 3H, OH, 5-CH & 6-CH), 1.75 (m, 1H, 6-CH), 1.98 – 2.06 (m, 2H, 8-CH & 2-CH), 2.25 (ddd, *J* = 11.8, 9.4 & 4.3 Hz, 1H, 5-CH), 4.17 (dddd, *J* = 9.6, 4.6, 3.1 & 1.6 Hz, 1H, 3-CH).

^{13}C NMR ($CDCl_3$, 125 MHz): δ 17.9, 18.3, 21.7, 25.3, 32.3, 37.3, 47.9, 74.9, 83.0, 90.4

GC-MS (*m/z*): 170 (M^+, 8), 137 (2), 128 (1), 127 (8), 125 (9), 111 (9), 109 (7), 97 (6), 95 (4), 87 (22), 86 (55), 71 (55), 43 (100).

HR-MS ($C_{10}H_{19}O_2$): Found 171.1374 (Calculated 171.1385).

Crystallography of 3α-hydroxy-1,4-cineole, **5f**, was performed as described in the supplementary material.

2.6 Synthesis of 1,4-cineole derivatives

3-keto-1,4-cineole 7b

A solution of tetrapropylammonium perruthnate (1.3 mg, 0.004 mmol) and 4-methylmorpholine N-oxide (10.1 mg, 0.086 mmol) in dry methylene chloride (0.25 ml) was added dropwise to a solution of 3-hydroxy-1,4-cineole (5 mg, 0.018 mmol) dissolved in dry methylene chloride (0.25 ml). The resulting mixture was stirred at room temperature for 1 hr before filtering through a silica plug and concentrating under a gentle stream of N_2 to give a clear oil (4.8 mg, 96%).

^{1}H NMR (500 MHz, $CDCl_3$): δ 2.22 (m, 2H, 6-CH_2), 2.18-2.12 (sept, *J* = 7 Hz, 1H, 8-CH), 1.88 (td, *J* = 12.4, 4.5 Hz, 1H, *ax* 3-CH), 1.80-1.75 (m, 1H, *ax* 2-CH), 1.74 – 1.65 (m, 1H, *eq* 2-CH), 1.64 – 1.57 (m, 1H, *eq* 3-CH), 1.55 (s, 3H, 7-CH_3), 1.06 (d, *J* = 6.9 Hz, 1H, 10-CH_3), 1.05 (d, *J* = 7.0 Hz, 1H, 9-CH_3).

^{13}C NMR (125 MHz, $CDCl_3$): δ 214.18, 91.85, 81.42, 51.24, 35.54, 28.29, 28.23, 21.54, 17.57, 17.35.

GC-MS (*m/z*): 168 (M^+, 1), 140 (30), 126 (18), 97 (18), 71 (100), 69 (64), 55 (25), 43 (88), 41 (44).

2-keto-1,4-cineole 7a

A solution of tetrapropylammonium perruthnate (1 mg, 0.003 mmol) and 4-methylmorpholine N-oxide (9.4 mg, 0.08 mmol) in dry methylene chloride (0.25 ml) was added dropwise to a solution of 3-hydroxy-1,4-cineole (1 mg, 0.006 mmol) dissolved in dry methylene chloride (0.25

ml). The resulting mixture was stirred at room temperature for 1 hr before filtering through a silica plug and concentrating under a gentle stream of N_2 to give a clear oil (1 mg, 100%).

GC-MS (*m/z*): 168 (M^+, 1), 140 (49), 107 (35), 97 (39), 83 (26), 69 (29), 55 (59), 43 (100), 41 (27)

8-dehydro-1,4-cineole 6

Freshly distilled $POCl_3$ (10 µL, 0.11 mmol) was added to a solution of 8-hydroxy-1,4-cineole (10 mg, 0.059 mmol) dissolved in pyridine (0.2 ml) before stirring for 24 hours at RT. The reaction as quenched with H_2O (1 ml) and extracted with ethyl acetate (2 x 1 ml). The organic layer was then washed with copper sulfate (2 x 1 ml), and brine (2 x 1 ml) before drying with magnesium sulfate and concentrating under a gentle stream of N_2 to afford the product as a clear oil (3 mg, 30%).

^{1}H NMR (500 MHz, $CDCl_3$): δ 4.98 (dq, *J* = 1.8, 0.9 Hz, 1H, 10-CH_2), 4.83 – 4.80 (m, 1H, 10-CH_2), 1.82 (dd, *J* = 1.5, 0.9 Hz, 3H, 9-CH_3), 1.81-1.66 (m, 9H, 2,3,5,6-CH_2) 1.49 (s, 3H, 7-CH_3).

GC-MS (*m/z*): 152 (M^+, 60), 123 (87), 109 (79), 79 (59), 69 (100), 67 (41), 43 (93), 41 (63).

3. Results

3.1 1,4-Cineole

Identification of the products of P450 catalysed oxidation of 1,4-cineole **2** was achieved by isolation and characterisation (NMR and mass spectrometry). *In vivo* oxidation reactions were used to prepare pure or highly enriched samples of **5a-f** (Scheme 2). These samples allowed identification of the products of *in vitro* turnover by GC-MS analysis via retention time and mass spectral fragmentation comparisons. In the case of **5f**, an X-ray structure was obtained for the product isolated from 1,4-cineole oxidation with F87W/Y96F/L244A (WFA) CYP101A1 and allowed the determination of its absolute configuration as (1*S*).

*3.1.1 CYP176A1 Oxidation: 1,4-Cineole **2***

CYP176A1 catalyses the selective oxidation of 1,8-cineole **1** to (1*R*)-6β-hydroxycineole **3a** and possesses a high binding affinity for 1,8-cineole (K_d = 0.7 μM) which also has the ability to induce a complete shift of the ferric heme from the low spin to the high spin form [42, 43]. Based on these properties of CYP176A1, 1,4-cineole was examined as a potential substrate. Binding studies were not possible with 1,4-cineole as it contains a small amount of 1,8-cineole that binds preferentially to CYP176A1 hindering quantitative analysis. Catalytic oxidation of 1,4-cineole by CYP176A1 generated two major products that were identified as 2β-hydroxy-1,4-cineole **5c** and 8-hydroxy-1,4-cineole **5a** (Fig. 3 and Scheme 2). Low levels of a third metabolite, which was assigned as 3β-hydroxy-1,4-cineole **5b**, was also detected (Fig. 3 and Scheme 2). Very low levels of a turnover product were also observed in the GC-MS and this was subsequently identified as **6** (*vide infra*).

*3.1.2 CYP101A1 Oxidation: 1,4-Cineole **2***

Two other enzymes, CYP101A1 and CYP102A1, and their mutants were then assessed to determine if these P450s could selectively oxidise 1,8- and 1,4-cineole. Firstly, WT

CYP101A1 oxidation of 1,4-cineole using a whole-cell system resulted in low yields and non-selective oxidation (Fig. 4). The two major products observed were subsequently identified (*vide supra*) as 8-hydroxy-1,4-cineole **5a** and 3α-1,4-hydroxycineole **5f**. However, mutants of CYP101A have been used to improve the yield and selectivity of monoterpene oxidation as was demonstrated with pinene and limonene [37, 51]. A library of eighteen members of CYP101A1 mutant enzymes (Table S1), member of which have been screened for the oxidation of terpenes and other hydrophobic substrates and have been cloned into a whole-cell oxidation system along with the physiological electron transfer partners, Pdx and PdR, was screened for selective catalysts for 1,4-cineole oxidation [37, 51, 52, 55, 101, 102].

Oxidation of 1,4-cineole with select CYP101A1 mutants improved the product yields and several showed high levels of regioselectivity. The CYP101A1 F87W/Y96F/L244A (WFA) mutant was greater than 90% selective for oxidation at the 3α position **5f** (Fig. 4, Scheme 2). This product was isolated in pure form and an X-ray structure of a single crystal not only confirmed its relative configuration but also revealed its absolute configuration as (1*S*). The optical rotation of the isolated product indicated that the bulk material was indeed significantly optically enriched ($[\alpha]_D^{23}$ 17°, lit. [100] $[\alpha]_D$ 2.5°; see supplementary material for more details). Several minor products were identified based on their MS fragmentation pattern, NMR spectra, and GC-MS retention time comparison with authentic standards (*vide supra*). These included 2α- **5e**, 2β- **5b**, 3β- **5c**, 8-hydroxy- **5a**, 9-hydroxy- **5d** and 3-keto-1,4-cineole **7b** (the latter only from large scale whole-cell turnovers) (Fig. 4, Experimental and Supplementary material).

The F87L/Y96F (LF) variant switched the selectivity of 1,4-cineole oxidation to favour (<85%) hydroxylation on the isopropyl substituent to give 8-hydroxy-1,4-cineole **5a** (Fig. 4, Scheme 2). Minor products were assigned as 2β- **5b**, 2α- **5e**, 9-hydroxy- **5d** and 2-keto-1,4-cineole **7a** (the latter only from large scale whole-cell turnovers) (Fig. 4,

Experimental and Supplementary material). In addition, there was also a significant increase in the minor metabolite at 4.15 min which possesses a MS consistent with a desaturation product (Fig. 4). Given that the increased level of this metabolite correlated with an increase in 8-hydroxy-1,4-cineole **5a** production across the range of mutants tested, we tentatively assigned this as the alkene between the C8 and C9 of 1,4-cineole **6** (Scheme 2). A standard sample of **6** was synthesised from **5a** by dehydration with $POCl_3$/pyridine and used to confirm the structure of this metabolite by comparison of GC-MS retention time and fragmentation pattern.

*3.1.3 CYP102A1 Oxidation: 1,4-Cineole **2***

The second enzyme that was examined for specific oxidation of 1,4- and 1,8-cineole was CYP102A1. CYP102A1 and different variants of CYP102A1 (6 variants in total, details in Table S1) tested for 1,4- and 1,8-cineole oxidation [83, 94]. The addition of polyfluorinated carboxylic acid decoy molecules (PFCs) as a method to improve the activity was also investigated [66, 94, 103-105]. The activity of WT CYP102A1 for both cineoles was low (Product Formation Rate (PFR); < 0.2 nmol(nmol-CYP)$^{-1}$min^{-1}; henceforth abbreviated to min^{-1}). The rate accelerating mutants and the use of the PFC decoy molecules did not significantly enhance the oxidation of either cineole (data not shown; these combination had previously been shown to improve the activity of alkylbenzenes and cycloalkanes) [66, 94]. Only variants that contained a mutation at the F87 active site residue showed significant product formation for either cineole (Fig. 5).

The CYP102A1 R47L/Y51F/A74G/F87V/L188Q (RLYFGVQ) and the A74G/F87V/L188Q (GVQ) variants improved the oxidation of 1,4-cineole, as compared to wild type, but two products were formed in roughly equal amounts and arose from hydroxylation at the 2α **5e** and the 3α **5f** positions (Fig. 5 and Scheme 2). The CYP102A1 R47L/Y51F/F87A/I401P (RLYFAIP) variant essentially generated 3α-hydroxy-1,4-cineole

5f as a single product (>90%). The PFR of 529 ± 48 min^{-1} (Table S2) was significantly faster than with any of the other CYP102A1 variants that were tested with 1,4-cineole. This presumably arises as the extra space created by the F87A mutation creates more space for the cineole to bind closer to the heme. Two minor products were formed in roughly equal amounts and these arose from hydroxylation at the 3β **5c** and 2α **5e** positions.

3.2 1,8-Cineole 1

3.2.1 CYP101A1 Oxidation

Previously we have shown that CYP101A1 from a *P. putida* was able to oxidise 1,8-cineole **1** to generate three major products; (1*S*)-6α- **3b** and 5α- **3c** and 5β-hydroxycineole **3d** in a 18:68:14 ratio. The latter two metabolites were also enriched in the (1*S*) enantiomer. A small amount of the 5-ketocineole **4** product was also generated (Fig. 6). In this study, the WT CYP101A1 oxidation of 1,8-cineole was found to be consistent with that reported previously (Fig. 6) [40]. The results obtained from screening the mutant libraries revealed that the selectivity of 1,8-cineole oxidation was altered in different CYP101A1 variants. For example the F87V/Y96F/L244A (VFA) variant showed a strong preference for oxidation at the 6α position (90%) to give (1*S*)-6α-hydroxycineole **3b** in essentially >99% e.e. Hydroxylation at the 5α and β positions made up the remainder of the observed products (8% and 2%, respectively, Fig. 6, Scheme 3). The F87W/Y96F/L244A/V247A (WFAL) variant hydroxylated 1,8-cineole to generate 5α-hydroxy-1,8-cineole **3c** as the major product (88%) with the minor products consisting of 6α-hydroxy-1,8-cineole **3b** (10%) and 5β-hydroxy-1,8-cineole **3d** (2%, Fig. 6, Scheme 2). The WFA variant was again more selective for oxidation at the 5α position (**3c**, 90%) with only 5β **3d** being detected as the minor product but the overall yield was lower (Fig. 6, Scheme 2). The optical purity of the 5-hydroxycineoles could not be determined directly by enantioselective GC [9, 40]. However, oxidation to the 5-ketocineole **4** allowed analysis by enantioselective GC and showed that

the major compound from the WFAL variant produced was the (1*S*) enantiomer in 86% e.e. The other mutants tested either resulted in lower yields or poorer selectivity after GC/GC-MS analysis (data not shown).

3.2.2 CYP102A1 Oxidation

The catalytic turnover of 1,8-cineole with WT CYP102A1 produced extremely small quantities of oxidation products. However, the CYP102A1 RLYFGVQ mutant with 1,8-cineole generated 6α-hydroxy-1,8-cineole **3b** as a single product (>98%), as did the GVQ mutant), with a PFR of 103 ± 25 min^{-1} (Fig. 5, Scheme 3 and Table S2). Enantioselective GC analysis indicated that this was again the (1*S*) isomer in 78% e.e.. The RLYFAIP variant was less selective for oxidation of 1,8-cineole generating significant quantities of 5α-hydroxy-1,8-cineole **3c** alongside the major product 6α-hydroxy-1,8-cineole **3b** (Fig. 5). The 5β-hydroxy metabolite **3d** made up the majority of the remainder of the oxidised 1,8-cineole.

3.3 Comparison of different bacterial P450 systems for cineole oxidation

Bacterial P450 enzyme systems are currently preferably used for biocatalytic reactions due to their ease of production and high activity levels. The use of whole-cell oxidation systems is a convenient method to generate larger scale quantities of metabolites. A direct comparison of the three systems studied here is complex due to differing requirements in cofactor usage (NADPH vs. NADH), electron transfer partner systems (ferredoxin vs. flavodoxin, fused single systems vs. three component system) and plasmid systems (pCWori+ bicistronic and tricistronic vs. pET28 systems). However, it is useful to compare the relative amount of product obtained for the most selective systems for 1,4- and 1,8-cineole oxidation. All the samples were tested in BL21(DE3) cells.

All the systems generated similar levels of cell biomass (13-16 grams of cell wet weight per litre of culture). The amount of P450 detected in the tricistronic CYP101A1

systems (10 – 97 nM) was generally lower than for the CYP102A1 systems (86 – 107 nM, Table S3). There was greater variation in the amount of P450 in each of the CYP101A1 systems, with, for example, the LF variant (97 nM) being formed in significantly greater quantities than either the WFA or VFA mutants (10 - 14 nM, Table S3).

After 16 hours of reaction, the level of 6α-hydroxy-1,8-cineole **3b** formed with the GVQ and RLYFGVQ CYP102A1 variant was ~2.25 ± 0.4 mM (4 mM substrate was added in total to each turnover). The RLYFFAIP variant generated 3α-hydroxy-1,4-cineole **5f** at similarly high levels (2.0 ± 0.1 mM when tested under the same conditions). In line with the lower levels of P450 production, the amount of hydroxylated metabolites were lower in the CYP101A1 whole-cell oxidation reactions. The LF variant system generated 470 μM 8-hydroxy-1,4-cineole **5a** (plus additional minor products), while the WFA variant generated up to 1 mM of 3α-hydroxy-1,4-cineole **5f** from 1,4-cineole. The VFA CYP101A1 variant produced 1 mM of 6α-hydroxy-1,8-cineole **3b** metabolite but the levels of the 5α hydroxylated 1,8-cineole **3c** formed by the WFA variant were considerably lower (~250 μM). For comparison, the amount of (1*R*)-6β-hydroxy-1,8-cineole **3a** generated using the CYP176A1 whole-cell oxidation system under the same conditions was ~650 μM. This could potentially be due to low levels of the endogenous *E. coli* flavodoxin reductase which is used in this system to transfer electrons from NADPH to cindoxin.

Overall the whole-cell turnover of the cineoles with the CYP102A1 variants seems to be better than with CYP101A1 variants. With 1,8-cineole the WT CYP101A1 system could generate similar levels of the mixture of the three hydroxyl cineoles formed (> 2.5 mM) suggesting that with further optimisation either system could be used for larger scale selective metabolite generation (Fig. 6).

4. Discussion

The ability to use engineered variants of the metalloproteins CYP101A1 and CYP102A1 to alter the regioselectivity of 1,8- and 1,4-cineole hydroxylation could lead to new routes for enantioselectively functionalised cineole analogues. The isolated CYP176A1 enzyme and a *Rhodococcus* bacterium have been reported to be capable of the preparative enantioselective oxidation of 1,8-cineole to (1*R*)-6β-hydroxy-1,8-cineole **3a** [9, 42]. The non-selective oxidation of 1,4-cineole by this enzyme and the fact that small levels of 1,8-cineole impurities preferentially bind to enzyme over the 1,4-analogue, highlights that CYP176A1 has evolved for the selective binding and oxidation of 1,8-cineole. This is perhaps unsurprising as this enzyme is responsible for the first step in the utilisation of 1,8-cineole as a carbon source. (1*R*)-6α-Hydroxy-1,8-cineole **3b** formation has also been reported from the oxidation of 1,8-cineole by *Bacillus cereus* [106]. A number of regioselective transformations of 1,8-cineole have also been reported but without any enantioselectivity data. For example, 6α-hydroxy-1,8-cineole **3b** is generated from biotransformations using the fungi *Cladosporium cladosporioides* [9]. Mixtures of products are reported for other biological oxidations of 1,8-cineole and 1,4-cineole [9].

Importantly, from screening just a small library of mutants, regioselective (and in some cases enantioselective) catalysts for the production of compounds arising from oxidation at the C3 and the C8 positions of 1,4-cineole and the C5 and C6 positions of 1,8-cineole were obtained in this study. This significantly expands upon the range of metabolites which can be selectively generated from 1,4- and 1,8-cineole using biotransformations. For both 1,4-and 1,8-cineole there was a preference for the CYP101A1 and CYP102A1 variants for oxidation on the α (or *endo*) face of the substrate whereas CYP176A1 is unusual in that it shows a preference for the *exo* (or β) face. The *endo* face would be considered to be less sterically hindered in both substrates. In CYP176A1 there is a specific hydrogen bond

between its asparagine 242 and the ether oxygen of 1,8-cineole which helps orientate the substrate for hydroxylation at a specific C-H bond (Fig. 2); mutation of this residue results in a significant increase in oxidation from the *endo* face [40].

For 1,8-cineole, CYP176A1 specifically generates the (1*R*)-6-hydroxycineole enantiomeric series whilst the CYP101A1 and CYP102A1 mutants found here generate the complementary (1*S*)-6-hydroxycineole series in good to excellent e.e. Two different CYP101A1 mutants were able to selectively hydroxylate the C5 position of 1,8-cineole with the WFA mutant yielding the (1*S*) compounds in high e.e. A lack of standards prevented complete determination of the enantiomeric purity of the hydroxycineoles produced from 1,4-cineole oxidation except in the case of **5f** formed via CYP101A1 mediated oxidation which was shown crystallographically to be the (1*S*) isomer in good e.e.

A significant improvement in yield as well as specificity was achieved for both the best CYP102A1 mutants. The small-scale CYP101A1 mutant screens produced catalysts with enhanced selectivity for metabolites including the enantiospecific production of the 6α– and 5α– isomers. The CYP101A1 LF mutant, which produces enhanced levels of the desaturated alkene product of 1,4-cineole **6**, will be a useful starting point for mutations to specific catalysts of this unusual P450 catalysed transformation.

Using CYP101A1 and CYP102A1 as biocatalysts has several advantages over isolating new enzymes. Both have been structurally characterised and the electron transfer proteins are well established. We have also shown that both systems are capable of oxidising cineole in good yields in non-optimised whole-cell oxidation systems in shake flasks. In addition, they have been extensively engineered and it has been shown that highly enantioselective hydroxylations are possible with evolved variants of both. Therefore, the variants of these enzymes used here will provide a good basis for further studies to enhance

the enantioselectivity, regioselectivity and activity of P450 catalysed biooxidations of cineole derivatives with these metalloenzymes.

1,4-Cineole Nomenclature Footnote

Nomenclature footnote: The nomenclature of the hydroxy 1,4-cineoles is relatively consistent within the literature but in IUPAC nomenclature the oxygen atom is labelled as position 7. However, this oxygen is frequently not assigned an atom number in the literature. To be consistent, we will employ the established literature numbering as shown. To discuss stereochemistry we have employed the descriptors α and β. The α descriptor is used to define the substituents that sit below the plane that passes through C2, C3, C5 and C6, while the β descriptor defines substituents above this plane. 1,4-Cineole is an achiral, *meso* compound; however, hydroxylation of either of the methylene bridges will produce enantiomeric compounds and generate three new stereogenic centres at C1, C4 and the hydroxylated carbon. Hence, a carbon atom that, following hydroxylation, generates the *R*-C1 isomer is defined as a pro-*R* carbon and a carbon atom that produces the *S*-C1 isomer is a pro-*S* carbon.

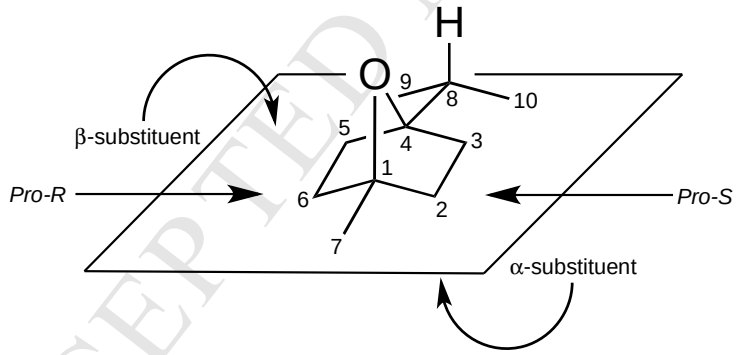

Acknowledgements

This work was in part supported by ARC grant DP140103229 (to JJDV and SGB). SGB acknowledges the ARC for a Future Fellowship (FT140100355). The authors also acknowledge the award of an Australian Government Research Training Program Scholarship (MPhil to JHZL). We than the Institute of Photonics and Advanced Sensing (IPAS, Adelaide) for supporting a Student Summer Scholarship (SAB). The authors thank Prof. Luet-Lok Wong (University of Oxford, UK) for the gene constructs of the CYP101A1 and CYP102A1 variants.

Abbreviations

P450, cytochrome P450; Cpd I, Compound I; CYP101A1, $P450_{cam}$; CYP102A1, $P450_{BM3}$; CYP176A1, $P450_{cin}$; Cdx, cindoxin; Pdx/PdR, [2Fe-2S] ferredoxin/flavin dependant ferredoxin reductase from *Pseudomonas putida*; VFA, CYP101A1 F87V/Y96F/L244A mutant; LF, CYP101A1 F87L/Y96F; VFA, CYP101A1 F87V/Y96F/L244A; AFA, CYP101A1 F87A/Y96F/V247A; GVQ, CYP102A1 A74G/F87V/L188Q; RLYFGVQ, CYP102A1 R47L/Y51F/A74G/F87V/L188Q; RLYFAIP, CYP102A1 R47L/Y51F/F87A/I401P; PFR, Product Formation Rate; FAD, flavin adenine dinucleotide; FMN, flavin mononucleotide; EMM, *E. coli* minimal media; PFC, perfluorocarboxylic acid; IPTG, Isopropyl β-D-1-thiogalactopyranoside; WT, wild-type.

References

[1] M. Ashour, M. Wink, J. Gershenzon, Annual Plant Reviews Volume 40: Biochemistry of Plant Secondary Metabolism, Wiley-Blackwell, 2010, pp. 258-303.
[2] J.S. Dickschat, Nat Prod Rep 33 (2016) 87-110.
[3] J. Schrader, in: R.G. Berger (Ed.), Flavours and Fragrances: Chemistry, Bioprocessing and Sustainability, Springer Berlin Heidelberg, Berlin, Heidelberg, 2007, pp. 507-574.
[4] C.A. Black, M. Parker, T.E. Siebert, D.L. Capone, I.L. Francis, Aust J Grape Wine Res 21 (2015) 582-600.
[5] F. Bakkali, S. Averbeck, D. Averbeck, M. Idaomar, Food Chem Toxicol 46 (2008) 446-475.
[6] M.C. Chang, J.D. Keasling, Nature chemical biology 2 (2006) 674-681.
[7] J. Mi, H. Schewe, M. Buchhaupt, D. Holtmann, J. Schrader, World J Microbiol Biotechnol 32 (2016) 112.
[8] L.C.A. Barbosa, C.A. Filomeno, R.R. Teixeira, Molecules 21 (2016).
[9] R. Azerad, ChemPlusChem 79 (2014) 634-655.
[10] E.S. Kovats, Helv Chim Acta 46 (1963) 2705-&.
[11] R.M. Carman, I.C. Macrae, M.V. Perkins, Aust J Chem 39 (1986) 1739-1746.
[12] Y. Asakawa, M. Toyota, T. Ishida, Xenobiotica; the fate of foreign compounds in biological systems 18 (1988) 1129-1134.
[13] A.F. Barton, B. Dell, A.R. Knight, J Agric Food Chem 58 (2010) 10147-10155.
[14] J.-A.M. Rasmussen, K.A. Henderson, M.J. Straffon, G.J. Dumsday, J. Coulton, M. Zachariou, Aus J Chem 58 (2005) 912-916.
[15] I.C. Macrae, V. Alberts, R.M. Carman, I.M. Shaw, Aust J Chem 32 (1979) 917-922.
[16] R.M. Carman, W.T. Robinson, C.J. Wallis, Aust J Chem 58 (2005) 785-791.
[17] W. Liu, J.P. Rosazza, Appl Environ Microbiol 59 (1993) 3889-3893.
[18] J.P. Rosazza, J.J. Steffens, F.S. Sariaslani, A. Goswami, J.M. Beale, S. Reeg, R. Chapman, Appl Environ Microbiol 53 (1987) 2482-2486.
[19] M. Miyazawa, Y. Hashimoto, J Agric Food Chem 50 (2002) 3522-3526.
[20] M. Miyazawa, M. Shindo, T. Shimada, Drug Metab Dispos 29 (2001) 200-205.
[21] R. Marmulla, J. Harder, Frontiers in microbiology 5 (2014) 346.
[22] J.L. Bicas, A.P. Dionísio, G.M. Pastore, Chem Rev 109 (2009) 4518-4531.
[23] H. Schewe, M.A. Mirata, J. Schrader, Adv Biochem Eng Biotechnol 148 (2015) 251-286.
[24] K.E. Slessor, D.B. Hawkes, A. Farlow, A.G. Pearson, J.E. Stok, J.J. De Voss, J Mol Catal B: Enzym 79 (2012) 15-20.
[25] M.J. Cryle, J.E. Stok, J.J. De Voss, Aust J Chem 56 (2003) 749-762.
[26] F.P. Guengerich, Chem Res Toxicol 14 (2001) 611-650.
[27] P.R. Ortiz de Montellano (Ed.), Cytochrome P450: Structure, Mechanism, and Biochemistry Springer International Publishing, Switzerland, 2015.
[28] S.G. Bell, L.L. Wong, in: M. Sono, J.H. Dawson (Eds.), Encyclopedia of Inorganic Chemistry **2005**.
[29] F. Hannemann, A. Bichet, K.M. Ewen, R. Bernhardt, Biochimica et biophysica acta 1770 (2007) 330-344.
[30] A.W. Munro, H.M. Girvan, K.J. McLean, Biochimica et biophysica acta 1770 (2007) 345-359.
[31] T.L. Poulos, Chem Rev 114 (2014) 3919-3962.
[32] J. Rittle, M.T. Green, Science 330 (2010) 933-937.
[33] J.T. Groves, G.A. McClusky, J Am Chem Soc 98 (1976) 859-861.

[34] V.B. Urlacher, S.G. Bell, L.L. Wong, in: R.D. Schmid, V.B. Urlacher (Eds.), Modern Biooxidation, Wiley, New York, **2007**, pp. 99-122.
[35] G.D. Roiban, M.T. Reetz, Chem Commun 51 (2015) 2208-2224.
[36] V.B. Urlacher, M. Girhard, Trends Biotechnol 30 (2012) 26-36.
[37] S.G. Bell, X. Chen, R.J. Sowden, F. Xu, J.N. Williams, L.L. Wong, Z. Rao, J Am Chem Soc 125 (2003) 705-714.
[38] J. Dietrich, Y. Yoshikuni, K. Fisher, F. Woolard, D. Ockey, D. McPhee, N. Renninger, M. Chang, D. Baker, J.D. Keasling, ACS Chem Biol 4 (2009) 261-267.
[39] R.J. Sowden, S. Yasmin, N.H. Rees, S.G. Bell, L.L. Wong, Org Biomol Chem 3 (2005) 57-64.
[40] J.E. Stok, E.A. Hall, I.S.J. Stone, M.C. Noble, S.H. Wong, S.G. Bell, J.J. De Voss, Journal of Molecular Catalysis B-Enzymatic 128 (2016) 52-64.
[41] R.J. Branco, A. Seifert, M. Budde, V.B. Urlacher, M.J. Ramos, J. Pleiss, Proteins 73 (2008) 597-607.
[42] D.B. Hawkes, G.W. Adams, A.L. Burlingame, P.R. Ortiz de Montellano, J.J. De Voss, J Biol Chem 277 (2002) 27725-27732.
[43] J.E. Stok, K.E. Slessor, A.J. Farlow, D.B. Hawkes, J.J. De Voss, Adv Exp Med Biol 851 (2015) 319-339.
[44] D.B. Hawkes, K.E. Slessor, P.V. Bernhardt, J.J. De Voss, Chembiochem 11 (2010) 1107-1114.
[45] K.E. Slessor, A.J. Farlow, S.M. Cavaignac, J.E. Stok, J.J. De Voss, Arch Biochem Biophys 507 (2011) 154-162.
[46] J.E. Stok, S. Yamada, A.J. Farlow, K.E. Slessor, J.J. De Voss, Biochim Biophys Acta Prot Proteom 1834 (2013) 688-696.
[47] Y.T. Meharenna, H. Li, D.B. Hawkes, A.G. Pearson, J. De Voss, T.L. Poulos, Biochemistry 43 (2004) 9487-9494.
[48] T.L. Poulos, B.C. Finzel, A.J. Howard, J Mol Biol 195 (1987) 687-700.
[49] J.A. Peterson, M.C. Lorence, B. Amarneh, J Biol Chem 265 (1990) 6066-6073.
[50] M.J. Honeychurch, A.O. Hill, L.L. Wong, FEBS letters 451 (1999) 351-353.
[51] S.G. Bell, R.J. Sowden, L.-L. Wong, Chem Commun (2001) 635-636.
[52] D.P. Nickerson, C.F. Harford-Cross, S.R. Fulcher, L.L. Wong, FEBS letters 405 (1997) 153-156.
[53] S.G. Bell, C.F. Harford-Cross, L.-L. Wong, Protein Eng 14 (2001) 797-802.
[54] S.G. Bell, N. Hoskins, C.J.C. Whitehouse, L.L. Wong, Met Ions Life Sci (**2007**) 437-476.
[55] F. Xu, S.G. Bell, Z. Rao, L.L. Wong, Protein Eng Des Sel 20 (2007) 473-480.
[56] K. Sakurai, H. Shimada, T. Hayashi, T. Tsukihara, Acta Crystallogr Sect F Struct Biol Cryst Commun 65 (2009) 80-83.
[57] C.F. Harford-Cross, A.B. Carmichael, F.K. Allan, P.A. England, D.A. Rouch, L.L. Wong, Protein Eng 13 (2000) 121-128.
[58] J.P. Jones, E.J. O'Hare, L.L. Wong, Eur J Biochem 268 (2001) 1460-1467.
[59] F. Xu, S.G. Bell, J. Lednik, A. Insley, Z. Rao, L.-L. Wong, Angew Chem Int Ed Engl 44 (2005) 4029-4032.
[60] A. Eichler, L. Gricman, S. Herter, P.P. Kelly, N.J. Turner, J. Pleiss, S.L. Flitsch, Chembiochem 17 (2016) 426-432.
[61] O. Sibbesen, Z. Zhang, P.R. Ortiz de Montellano, Arch Biochem Biophys 353 (1998) 285-296.
[62] P.P. Ho, A.J. Fulco, Biochimica et biophysica acta 431 (1976) 249-256.
[63] C.J. Whitehouse, S.G. Bell, L.L. Wong, Chem Soc Rev 41 (2012) 1218-1260.
[64] H. Li, T.L. Poulos, Nat Struct Biol 4 (1997) 140-146.

[65] K.Y. Choi, E. Jung, D.H. Jung, B.P. Pandey, H. Yun, H.Y. Park, R.J. Kazlauskas, B.G. Kim, FEBS J 279 (2012) 1650-1662.
[66] S.D. Munday, S. Dezvarei, S.G. Bell, ChemCatChem 8 (2016) 2789-2796.
[67] M. Dietrich, S. Eiben, C. Asta, T.A. Do, J. Pleiss, V.B. Urlacher, Appl Microbiol Biotechnol 79 (2008) 931-940.
[68] M. Budde, S.C. Maurer, R.D. Schmid, V.B. Urlacher, Appl Microbiol Biotechnol 66 (2004) 180-186.
[69] M.C. Gustafsson, O. Roitel, K.R. Marshall, M.A. Noble, S.K. Chapman, A. Pessegueiro, A.J. Fulco, M.R. Cheesman, C. von Wachenfeldt, A.W. Munro, Biochemistry 43 (2004) 5474-5487.
[70] S.D. Munday, N.K. Maddigan, R.J. Young, S.G. Bell, Biochimica et biophysica acta 1860 (2016) 1149-1162.
[71] M.G. Joyce, I.S. Ekanem, O. Roitel, A.J. Dunford, R. Neeli, H.M. Girvan, G.J. Baker, R.A. Curtis, A.W. Munro, D. Leys, FEBS J 279 (2012) 1694-1706.
[72] T. Kitazume, D.C. Haines, R.W. Estabrook, B. Chen, J.A. Peterson, Biochemistry 46 (2007) 11892-11901.
[73] R. Neeli, H.M. Girvan, A. Lawrence, M.J. Warren, D. Leys, N.S. Scrutton, A.W. Munro, FEBS Lett. 579 (2005) 5582-5588.
[74] P. Meinhold, M.W. Peters, A. Hartwick, A.R. Hernandez, F.H. Arnold, Adv Synth Catal 348 (2006) 763-772.
[75] W.C. Huang, A.C. Westlake, J.D. Marechal, M.G. Joyce, P.C. Moody, G.C. Roberts, J Mol Biol 373 (2007) 633-651.
[76] S. Kille, F.E. Zilly, J.P. Acevedo, M.T. Reetz, Nat Chem 3 (2011) 738-743.
[77] G. Di Nardo, G. Gilardi, Int J Mol Sci 13 (2012) 15901-15924.
[78] R. Singh, M. Bordeaux, R. Fasan, ACS Catal 4 (2014) 546-552.
[79] R. Singh, J.N. Kolev, P.A. Sutera, R. Fasan, ACS Catal 5 (2015) 1685-1691.
[80] P.S. Coelho, E.M. Brustad, A. Kannan, F.H. Arnold, Science 339 (2013) 307-310.
[81] T.K. Hyster, C.C. Farwell, A.R. Buller, J.A. McIntosh, F.H. Arnold, J Am Chem Soc 136 (2014) 15505-15508.
[82] C.C. Farwell, R.K. Zhang, J.A. McIntosh, T.K. Hyster, F.H. Arnold, ACS Cent Sci 1 (2015) 89-93.
[83] C.J. Whitehouse, S.G. Bell, H.G. Tufton, R.J. Kenny, L.C. Ogilvie, L.L. Wong, Chem Commun (2008) 966-968.
[84] C.J. Whitehouse, S.G. Bell, W. Yang, J.A. Yorke, C.F. Blanford, A.J. Strong, E.J. Morse, M. Bartlam, Z. Rao, L.L. Wong, ChemBioChem 10 (2009) 1654-1656.
[85] C.J. Whitehouse, W. Yang, J.A. Yorke, B.C. Rowlatt, A.J. Strong, C.F. Blanford, S.G. Bell, M. Bartlam, L.L. Wong, Z. Rao, ChemBioChem 11 (2010) 2549-2556.
[86] C.J. Whitehouse, W. Yang, J.A. Yorke, H.G. Tufton, L.C. Ogilvie, S.G. Bell, W. Zhou, M. Bartlam, Z. Rao, L.L. Wong, Dalton Trans 40 (2011) 10383-10396.
[87] Q.S. Li, J. Ogawa, R.D. Schmid, S. Shimizu, FEBS letters 508 (2001) 249-252.
[88] Q.S. Li, J. Ogawa, R.D. Schmid, S. Shimizu, Appl Environ Microbiol 67 (2001) 5735-5739.
[89] G.D. Roiban, R. Agudo, A. Ilie, R. Lonsdale, M.T. Reetz, Chem Commun 50 (2014) 14310-14313.
[90] A. Seifert, S. Vomund, K. Grohmann, S. Kriening, V.B. Urlacher, S. Laschat, J. Pleiss, ChemBioChem 10 (2009) 853-861.
[91] Q.S. Li, U. Schwaneberg, P. Fischer, R.D. Schmid, Chem Eur J 6 (2000) 1531-1536.
[92] B. Unterweger, D.M. Bulach, J. Scoble, D.J. Midgley, P. Greenfield, D. Lyras, P. Johanesen, G.J. Dumsday, Appl Environ Microbiol 82 (2016) 6507-6517.

[93] G.E. Collis, B. Unterweger, G.J. Dumsday, C.M. Forsyth, Acta Crystallogr E Crystallogr Commun 73 (2017) 1242-1245.
[94] S.D. Munday, O. Shoji, Y. Watanabe, L.L. Wong, S.G. Bell, Chem Commun 52 (2016) 1036-1039.
[95] A.J. Farlow, P.V. Bernhardt, J.J. De Voss, Tetrahedron-Asymmetry 24 (2013) 324-333.
[96] T. Omura, R. Sato, J Biol Chem 239 (1964) 2370-2378.
[97] Y. Asakawa, R. Matsuda, M. Tori, T. Hashimoto, Phytochemistry 27 (1988) 3861-3869.
[98] R.M. Carman, A.C. Rayner, Aust J Chem 47 (1994) 2087-2097.
[99] R.M. Carman, A.C. Rayner, Aus. J. Chem. 47 (1994) 2087-2097.
[100] M. Miyazawa, Y. Noma, K. Yamamoto, Chemistry Express 7 (1992) 125 - 128.
[101] P.A. England, D.A. Rouch, A.C.G. Westlake, S.G. Bell, D.P. Nickerson, M. Webberley, S.L. Flitsch, L.L. Wong, Chem Commun (1996) 357-358.
[102] S.G. Bell, D.A. Rouch, L.-L. Wong, J Mol Catal B: Enzym 3 (1997) 293-302.
[103] N. Kawakami, O. Shoji, Y. Watanabe, Angew Chem Int Ed Engl 50 (2011) 5315-5318.
[104] O. Shoji, T. Kunimatsu, N. Kawakami, Y. Watanabe, Angew Chem Int Ed Engl 52 (2013) 6606-6610.
[105] Z. Cong, O. Shoji, C. Kasai, N. Kawakami, H. Sugimoto, Y. Shiro, Y. Watanabe, ACS Catal 5 (2015) 150-156.
[106] W.G. Liu, J.P.N. Rosazza, Tetrahedron Lett 31 (1990) 2833-2836.

Scheme 1 CYP176A1 mediated oxidation of **1** produces a single enantiomer (1*R*)-6β-hydroxy-1,8-cineole **3a**; CYP101A1 catalysed oxidation of **1** generates a mixture of isomers that include (1*S*)-6α-hydroxycineole **3b** and both enantiomers of 5α- and 5β-hydroxycineole **3c-d**. A small amount of over-oxidation was also observed producing both enantiomers of 5-ketocineole **4** [40].

Scheme 2 Products arising from the catalytic turnover of 1,4-cineole with: CYP176A1; CYP101A1 LF; CYP101A1 WFA; and CYP102A1 RLYFFAIP.

Scheme 3 Products arising from the turnover of 1,8-cineole with CYP101A1 and CYP102A1 their variants. For the WFAL and VFA mutant forms there were additional minor products (<1% total) with masses consistent with that of the 5-keto metabolite (**4**) and other hydroxylated and ketone products (data not shown).

Figure 1 Chemical structures of 1,8-cineole **1** and 1,4-cineole **2**.

Figure 2 (a) Active site of Cytochrome CYP176A1 P450cin with 1,8-cineole bound (PDB ID: 1T2B). The Asn242 residue has a hydrogen bonding interaction with the ether oxygen of 1,8-cineole. (b) Active site of Cytochrome CYP101A1 with camphor bound (PDB ID: 3WRH). (c) Active site of Cytochrome CYP102A1 (P450BM3) with palmitoleic acid bound (PDB ID: 1FAG). Residues of interest in this work are highlighted in cyan

Figure 3 GC-MS analysis of the *in vivo* turnover of 1,4-cineole **2** by CYP176A1. The substrates and products are labelled as follows; 1,4-cineole (4.0 min), 8-hydroxy-1,4-cineole **5a** (6.0 min; 8-hydroxy), 3β-hydroxy-1,4-cineole **5b** (6.85 min; 3β), 2β-hydroxy-1,4-cineole **5c** (7.15 min; 2β), 6β-hydroxy-1,8-cineole **3a** (7.5 min; 6β-1,8), which is present in the 1,4-cineole turnover due to 1,8-cineole impurity, (1,8- RT 4.3 min; 1,8). The desaturation product **6** is labelled (#, RT 4.15 min). A potential ketone metabolite of unknown origin was labelled. $ (m/z = 168.05, RT 7.1 min).

Figure 4 GC-MS analysis of the *in vivo* turnover of 1,4-cineole by different variants of CYP101A. The chromatograms have been offset along the y axis for clarity. From lowest to highest the variants are: WT CYP101A1; WFAL; and LF. The products are labelled as follows: 8-hydroxy-1,4-cineole **5a** (6.0 min; 8-hydroxy); 3β-hydroxy-1,4-cineole **5b** (6.85 min; 3β); 2β-hydroxy-1,4-cineole **5c** (7.15 min; 2β); 3α-hydroxy-1,4-cineole **5f** (7.3 min; 3α); 2α-hydroxy-1,4-cineole **5e** (7.65 min; 2α); and 9-hydroxy-1,4-cineole **5d** (8.25 min; 9-hydroxy). The 1,4-cineole desaturation product, **6**, has been labelled (#, 4.15 min). Impurities and products arising from the turnover of 1,8-cineole (1,8) have been labelled *. Note the WFA variants gives a similar distribution to WFAL but has been omitted from this graph for clarity.

Figure 5 GC-MS analysis of the *in vitro* turnover of 1,4-cineole (left) and 1,8-cineole (right) by different variants of CYP102A1. The chromatograms have been offset along the x and y axes for clarity. From lowest to highest the variants are for 1,4-cineole: WT CYP102A1 (light grey); R19 (grey); GVQ (dark grey); and RLYFFAIP (black). For 1,8-cineole they are: WT CYP102A1 (grey); RLYFFAIP (dark grey); and RLYFGVQ (black). The products are labelled as follows: 1,4-cineole; 3β-hydroxy-1,4-cineole **5b** (3β), 3α-hydroxy-1,4-cineole **5f** (3α), and 2α-hydroxy-1,4-cineole **5e** (2α); 1,8-cineole; 6α-hydroxy-1,8-cineole **3c** (6α), 5α-hydroxy-1,8-cineole **3b** (5α) and 5β-hydroxy-1,8-cineole **3d** (5β). Impurities have been labelled * and $. Note the retention times are slightly different to those reported previously due to the use of a different instrument/column.

Figure 6 GC-MS analysis of the *in vivo* turnover of 1,8-cineole by different variants of CYP101A1. In the top chromatogram is the turnover of 1,8-cineole by the WT CYP101A1 enzyme. The bottom graph is the analysis of the turnover of 1,8-cineole by the: VFA (grey solid line); WFAL (black line – dashes and dots); and WFA (black solid line) mutants. These chromatograms have been offset along the y axis for clarity. The products are labelled

as follows: 6α-hydroxy-1,8-cineole **3b** (RT 7.7 min; 6α); 5α-hydroxy-1,8-cineole **3c** (5α, RT 7.9 min; 5α); and 5β-hydroxy-1,8-cineole **3d** (RT 8.2 min; 5β).

Scheme 1

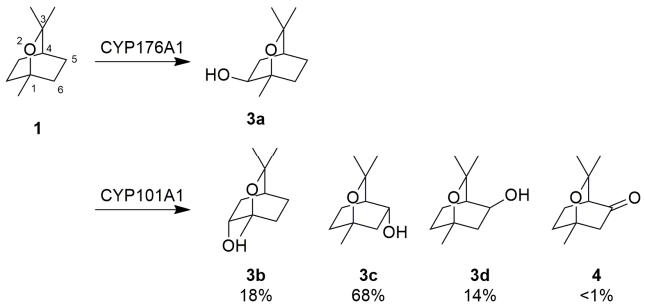

Scheme 2

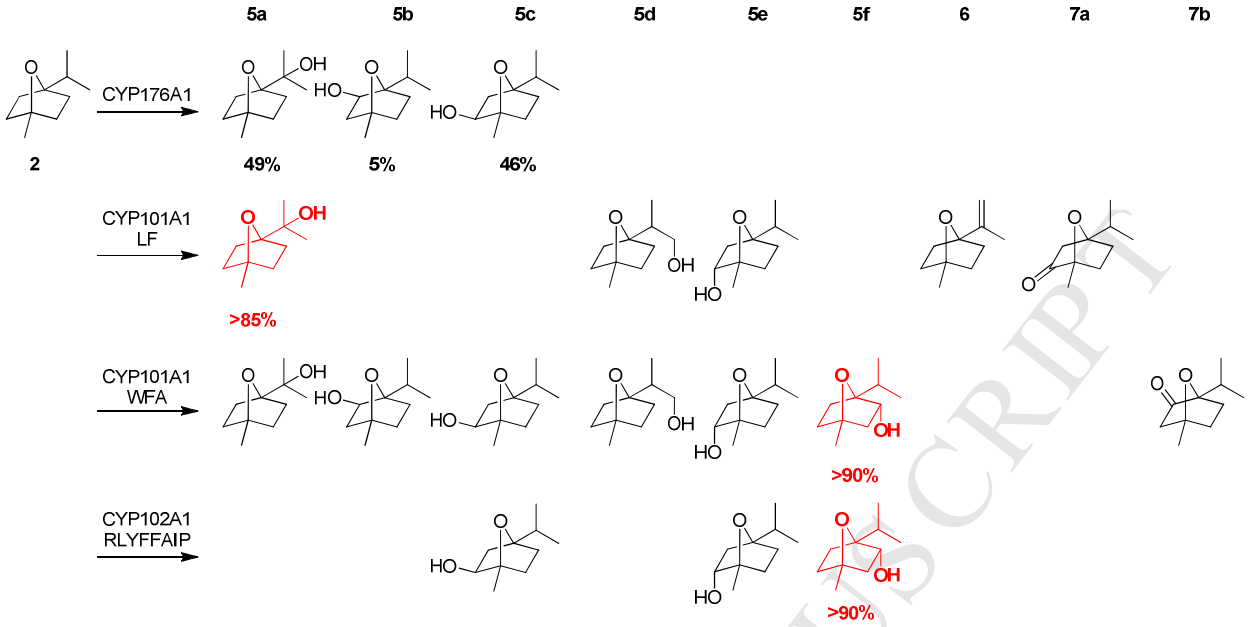

Scheme 3

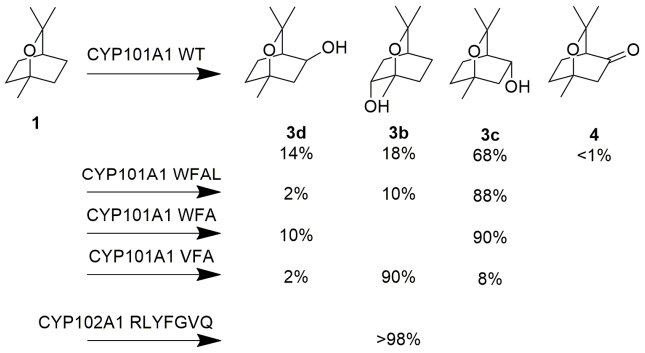

Figure 1

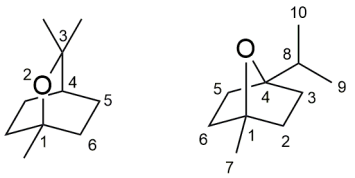

1,8-cineole **1** 1,4-cineole **2**

Figure 2

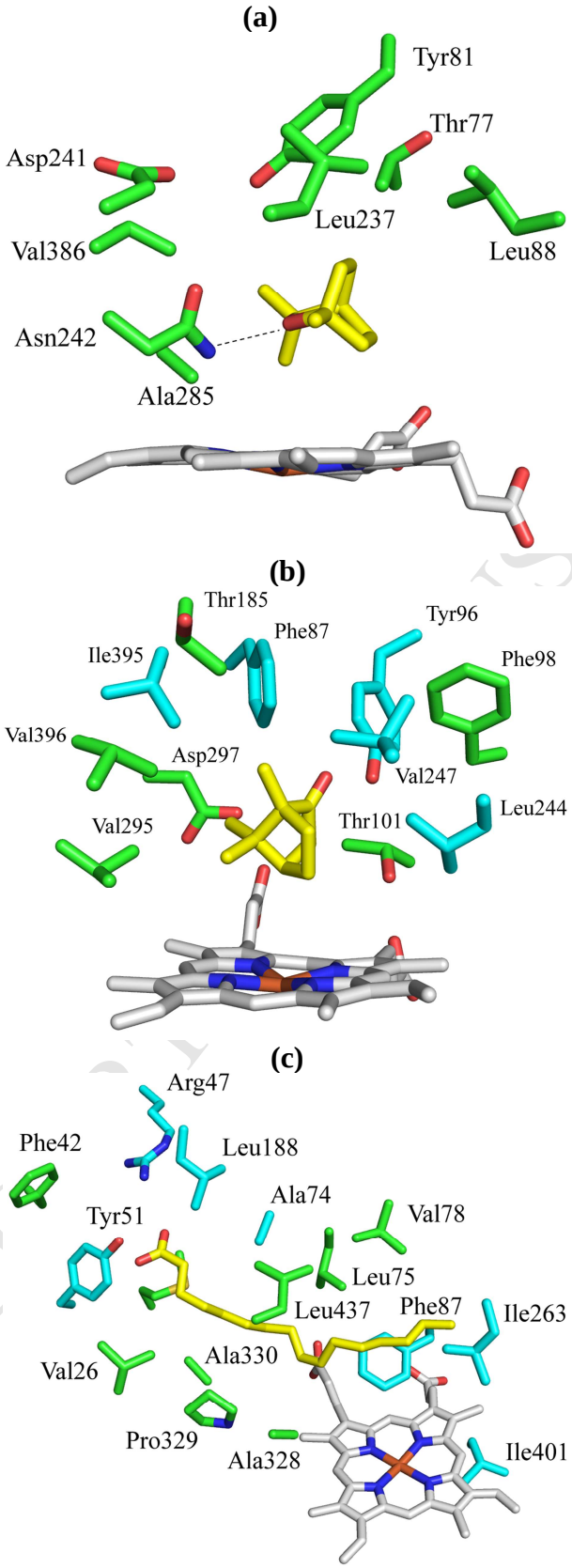
(a)
Tyr81
Thr77
Asp241
Leu237
Leu88
Val386
Asn242
Ala285
(b)
Thr185
Phe87
Tyr96
Ile395
Phe98
Val396
Asp297
Val247
Val295
Thr101
Leu244
(c)
Arg47
Phe42
Leu188
Ala74
Tyr51
Val78
Leu75
Leu437
Phe87
Ile263
Val26
Ala330
Pro329
Ala328
Ile401

Figure 3

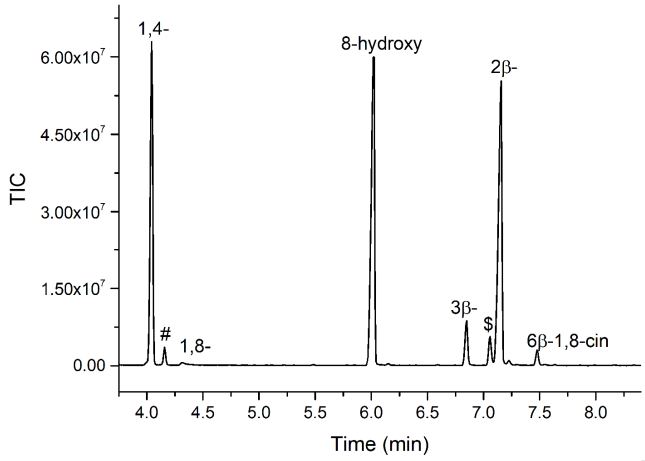

Figure 4

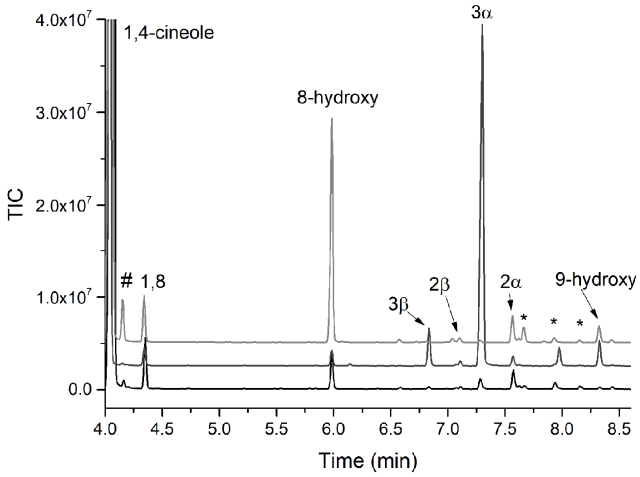

Figure 5

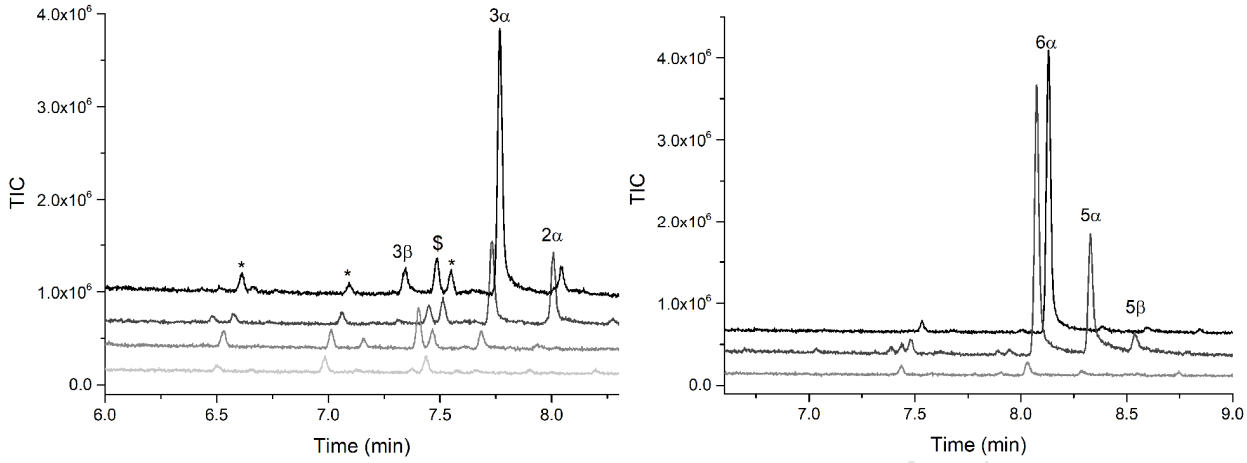

Figure 6